

A SELF-CONTROLLED MAGLEV SYSTEM

F. Di Puccio¹, A. Musolino^{2, *}, R. Rizzo², and E. Tripodi²

¹Department of Mechanical, Nuclear and Industrial Engineering, University of Pisa, Via Diotisalvi 2, Pisa 56126, Italy

²Department of Energy and System Engineering, Largo L. Lazzarino, Pisa 56123, Italy

Abstract—This paper presents a MAGLEV system in which the magnetic suspension is assured by the repulsion of permanent magnets both on the guideway and on the vehicle. Due to the induced currents on a aluminum sheath surrounding the magnets on the guideway, the system intrinsic instability is overcome. The detailed structure of the proposed system is described and the main results of the simulations by means a FE code are reported.

1. INTRODUCTION

MAGNETIC levitation (Maglev) uses magnetic forces to “levitate” vehicles at short distance from a dedicated guide, allowing a safe travel at speeds greater than 150 m/s (540 km/h) [1, 2]. Magnetic forces are also used for non-contact guidance and propulsion.

There exist two main types of magnetic levitation systems: the first is based on electromagnets [3, 4], the second on superconducting magnets [5, 6]. Both are complex and present various drawbacks.

The system based on electromagnets works in attraction mode and is able to produce an attraction force between the vehicle and the rails. A control system (which adjusts the electromagnet current) is needed to maintain a constant clearance between the vehicle and the rails [7, 8]. The main limitation of this system is the potential unreliability of the control system. Furthermore the electromagnets are very heavy and result in increased complexity and cost of the guideway.

In the second type of maglev system, the repulsive levitation force is obtained by the interaction between the field of moving

Received 10 September 2012, Accepted 12 October 2012, Scheduled 19 October 2012

* Corresponding author: Antonino Musolino (musolino@dsea.unipi.it).

superconducting magnets on the vehicle and the induced currents in the conductive track or coils in the guideway [9,10]. The main drawbacks are the complexity of the cooling (cryogenic) system of the superconducting coils, and the potentially high magnetic field in the passengers' compartment [11].

As an alternative to the previous systems, many authors attempted to develop maglev systems based on the natural repulsive force of two oppositely magnetized permanent magnets (PM) [12–16]. However these early studies have been set aside due to the intrinsic instability of passive magnetic systems, a direct consequence of Earnshaw's theorem (1842) [17] and Braunbeck's extension [18]. These theorems state that a body with steady charges, magnetizations, or current placed in a steady electric or magnetic field cannot rest in stable equilibrium under the action of electric and magnetic fields alone. The realization of passive MAGLEV systems based on PMs only is then prevented. However, to the point of view of a system engineer, an interesting aspect is to verify the existence of conditions characterized by small values of the ratio between the destabilizing forces and stabilizing ones [19–21].

In a Maglev system, the presence of bodies in motion suggests that the steady conditions on which Earnshaw and Braunbeck's theorems are based can be overcome and, therefore, it is possible to identify proper arrangements of PMs and conductive bodies in which, under the correct conditions [22], there are no unstable forces (unstable forces due to PMs are compensated by those due to motional induced eddy currents) [23]. Starting from this assumption and taking into account the recent improvements in PM materials [24], it is possible to design a passive maglev system for public transportation which has evident advantages over the existing ones [25].

The paper is organized as follows: Section 2 briefly reviews the more used numerical approaches for the numerical analysis of electromechanical devices. The analyzed system is described in detail in Section 3. The numerical results are shown and discussed in Section 4. Section 5 reports the analysis of the vehicle oscillations and Section 6 briefly evaluates the propulsion requirements.

2. CHOICE OF THE NUMERICAL FORMULATION

The analytical solution of the 3D diffusion equation in presence of moving conductors presents serious difficulties even in simple cases. When complex geometries and nonlinear materials are present, an accurate analysis can be performed by numerical methods only.

Differential and integral formulations are at the basis of the

most popular computational approaches: the Finite Element Method (FEM) and the Method of Moments (MoM) and their respective variations. FEM analysis is widely used since it allows modeling devices with complex shapes and characterized by nonlinear materials. The application of FEM to systems with moving conductors presents some difficulties due to the relative motion of the bodies and their own meshes. Despite the availability of commercial codes that are able to solve this problem [26, 27] the search for robust and efficient methods is still an open issue. Alternative approaches, mostly based on integral formulations [28–37], have a number of characteristics that make them well suited for the analysis of electromechanical devices. In particular integral formulations require the discretization of the active regions only and the problem of coupling meshes with different speed is absent. Furthermore integral formulations automatically satisfy the far-field boundary conditions and coarse discretization (with respect to those typically used in FEM) are able to provide good accuracy. MoM based approaches can often be reformulated in terms of equivalent networks whose coupling with external lumped circuits is straightforward. This is an important feature. In fact, the stabilization systems are constituted by electromagnets whose currents are provided by electronic circuits on the basis of real time control strategies. A simulation environment which allows evaluating the behavior of the system to stabilize together with the control devices and their drivers is a valuable aid to the design activities. Another opportunities related to the construction of an equivalent network is the availability of robust and efficient sensitivity analysis tools with respect to the design parameters which greatly helps in the development of the system [38, 39].

The simulations of the present work have been mainly carried out by the use of EFFE (former MEGA) [26]. This is a Finite Elements code formerly developed at University of Bath (UK) and commonly used in the analysis of electromechanical devices. It is able to take into account the B-H function for nonlinear materials, the relative movement between different bodies, the presence of PMs, as well as the transient behavior of the system. Furthermore, the EFFE software is able to analyze coupled electromagnetic-thermal problems.

3. THE PROPOSED SYSTEM

The basic idea of the proposed system is that it may be possible to overcome the intrinsic instability of PMs system exploiting the relative movement between the subparts of the system itself. As a consequence of the Laplace equation governing steady magnetic problems, we can

write $\nabla \cdot \bar{F} = 0$; i.e., the sum of the derivatives of forces F_x , F_y and F_z acting in passive permanent magnet system is zero:

$$\frac{\partial F_x}{\partial x} + \frac{\partial F_y}{\partial y} + \frac{\partial F_z}{\partial z} = 0 \Rightarrow \frac{\partial F_x}{\partial x} = - \left(\frac{\partial F_y}{\partial y} + \frac{\partial F_z}{\partial z} \right). \quad (1)$$

This means that not all the derivatives of the forces with respect to the displacement can be negative. At least one must be positive and this means that the system is unstable in this direction [18–20]. However, if parts of the system are in motion near conducting materials, eddy currents are induced and the system is not under the action of steady magnetic fields alone. The proposed system, able to exploit the motion induced eddy currents in order to achieve stability, is shown in Fig. 1. It is composed of two parts: a system of PMs properly positioned on to the guideway and surrounded by an aluminum sheath forms the rails; another arrangement of PMs only constitutes the levitated vehicle. The PMs are rare earth Nd-Fe-B magnets, with a remnant field B_r of 1.35 T, a coercivity H_{ci} of 880 kA/m and a maximum temperature operation of about 100°C. Fig. 2(a) shows the single rail system. It is composed of an aluminum hollow cylinder, extending along the whole path; inside it, an arrangement of PMs with proper shapes and direction of magnetization is located. Fig. 2(b) shows a single unit of the vehicle system. The unit contains only PMs with magnetization \bar{M} opposite to that of rail system.

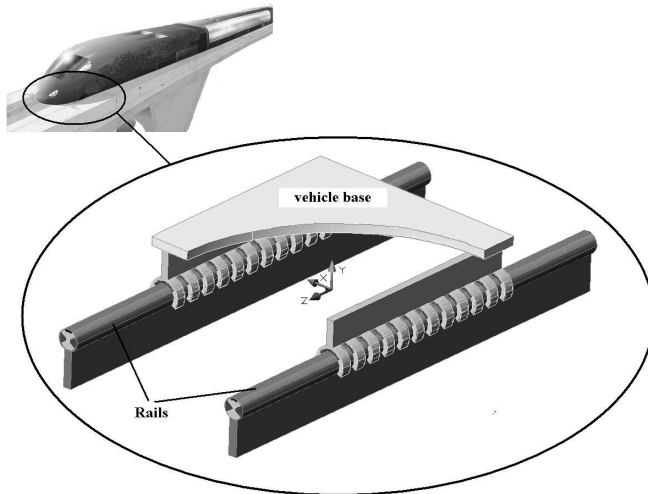


Figure 1. Schematic representation of the proposed system.

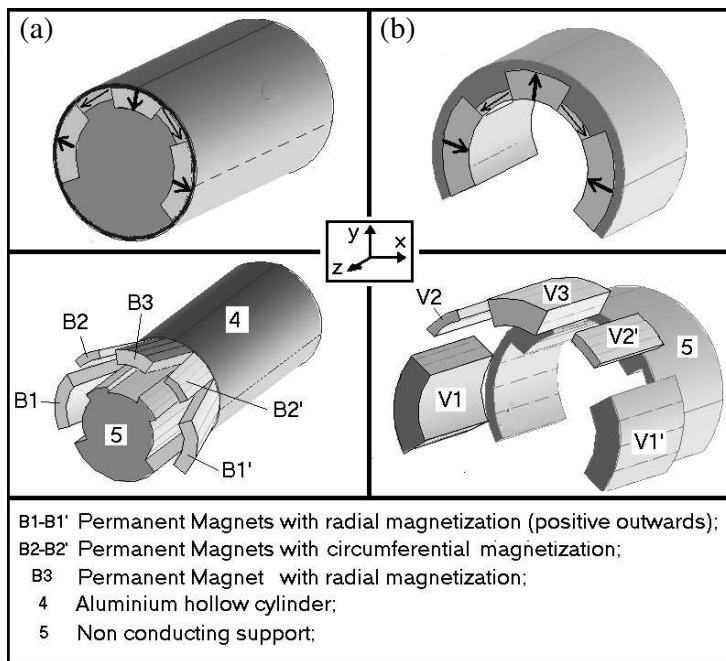


Figure 2. The vehicle and the rails subsystems.

The whole vehicle system is obtained by assembling together the correct number of single units calculated to counterbalance the weight of the load levitating at a distance of about 7.5 mm over the rails, and to achieve suitable stabilizing forces along x and y directions in order to ensure safe flight under destabilizing external effects (wind pressure, centrifugal forces, etc.). Since the distance between two consecutive units influences the force along z and x directions, these units need the correct separation from each other.

Figure 3 reports the system dimensions. In order to improve the behavior of the device, several simulations have been carried out by using as design criteria the maximization of the stiffness of the levitating and horizontal forces with a constant clearance value of 7.5 mm between the static and the moving subsystem.

Figure 4 shows the 3D mesh and a 2D slice through it, used to perform the FE analysis. Due to the symmetry of the system only half domain is analyzed; furthermore, due to the periodicity of the vehicle system along the z direction it is possible to reduce complexity of the model by means of the imposition of the periodic boundary conditions in the FE code.

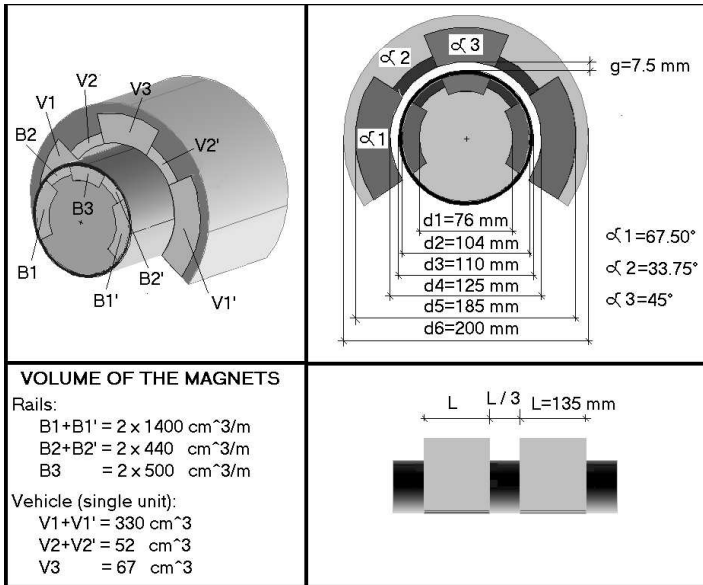


Figure 3. System dimensions adopted in the simulations.

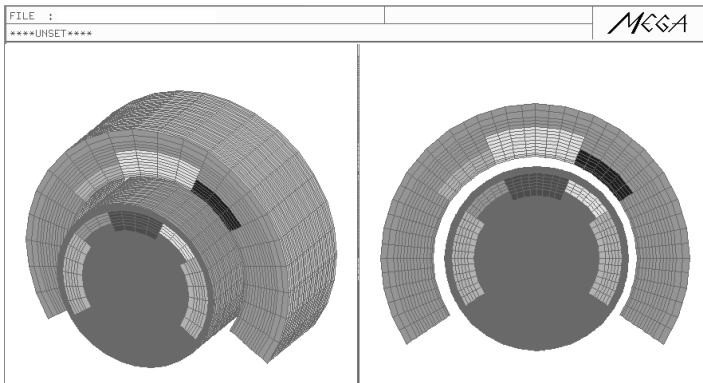


Figure 4. The 3D FE model mesh.

4. RESULTS AND DISCUSSION

The proposed system has been applied to a magnetically levitated a vehicle for transportation purposes at a cruise speed of 100 m/s. It has a capacity of 70 passengers and a full load mass M of 30000 kg. The vehicle dimensions are: length $L = 25$ m, width $W = 2.9$ m and height $H = 2.9$ m.

Since the guideway has two rails, the number of single units composing the vehicle is $125 \times 2 = 250$, placed along two parallel lines and symmetrically positioned as in Fig. 1.

Let us observe that because of the symmetry of the system along the z -direction, F_z and its stiffness are identically zero without the eddy currents.

However, the results hereafter reported refer to the single unit (shown in Fig. 2(b)) which makes up the vehicle system.

4.1. Simulation Results

Figure 5 shows the levitating force F_y as a function of the distance traveled on the rail and for different values of speed with the vehicle centered on its path. It can be seen that there is little difference between the values of force F_y with changes in speed; the system is able to levitate at zero speed.

Figure 6 shows the profile of force F_z (“magnetic drag force”) along the direction of motion. As expected, this force decreases as speed increases and its negative value must be taken into account in the design of the propulsion system. When the system is perfectly centered, no force along the x direction is present.

In order to analyze the conditions of stability along x and y directions, a set of simulations with the off centered system has been carried out. Fig. 7 shows the profile of the horizontal force F_x at different speeds as a function of the distance traveled by the vehicle and of the shift d_x of the vehicle from its centered trajectory.

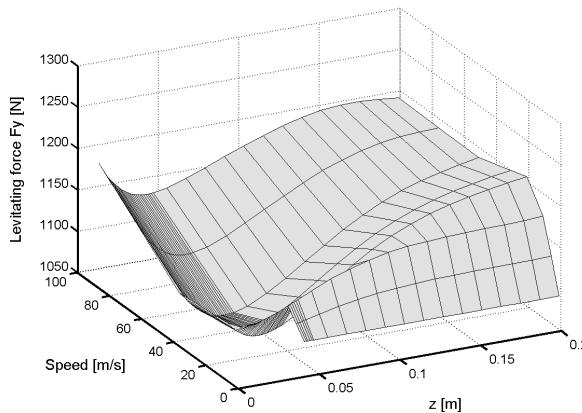


Figure 5. Levitation force F_y of a single unit as a function of the distance traveled by the vehicle in the z direction and of the speed.

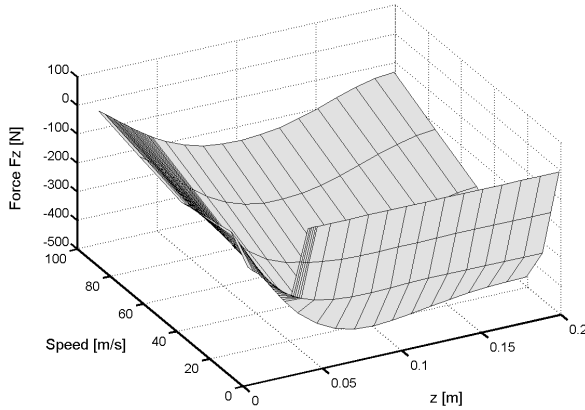


Figure 6. Drag force F_z of a single unit as a function of the distance traveled by the vehicle in the z direction and of the speed.

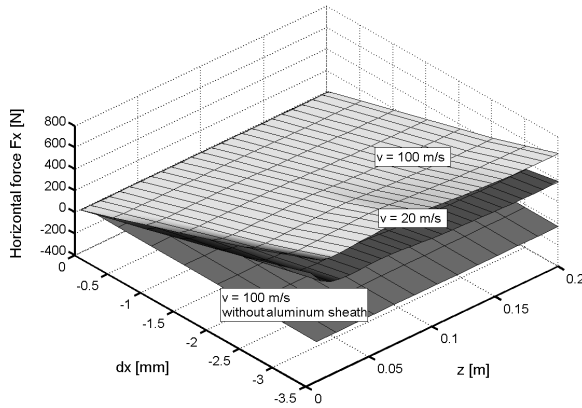


Figure 7. Force F_x of a single unit as a function of the distance traveled by the vehicle and of the shift d_x of the vehicle from its centered path.

Figure 8 shows the stiffness $\partial F_x / \partial dx$ of F_x . It can be seen that the system with the aluminum sheath is stable along the horizontal direction. Let us observe that if the induced currents are absent, the value of the force F_x , is very small with respect to the other forces in the system. Furthermore, if the shift d_x of the system is assumed to be smaller than half clearance, $d_x < g/2$, the stiffness of the whole system

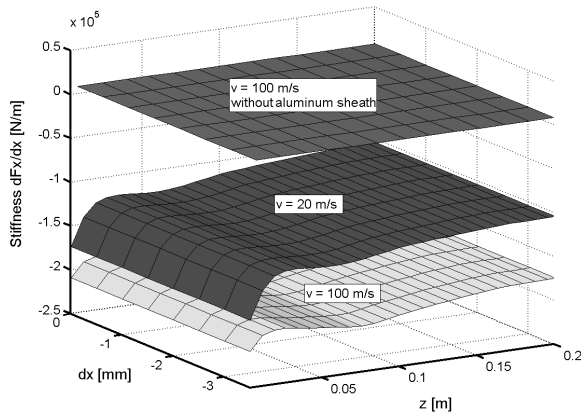


Figure 8. Stiffness $\partial F_x / \partial x$ of a single unit as a function of the distance traveled by the vehicle and of the its shift d_x from its centered path.

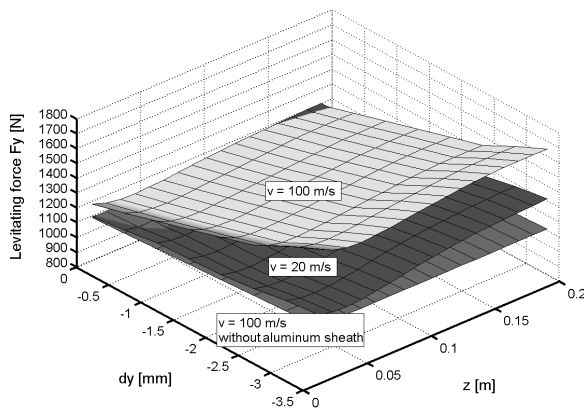


Figure 9. Levitation force F_y of a single unit at different speeds as a function of the distance traveled by the vehicle and its vertical shift d_y .

is almost constant, and at the design speed of 100 m/s, it exceeds the value -4×10^7 N/m (considering the total length of the vehicle).

Figures 9 and 10 respectively report the levitating force F_y and its stiffness $\partial F_y / \partial y$ as a function of the distance traveled by the vehicle and of the vertical shift d_y .

It can be seen that the value of the stiffness along this direction is: $\partial F_y / \partial y = -3.3 \times 10^7$ N/m at 100 m/s and that the system is stable along this direction also when it is stationary.

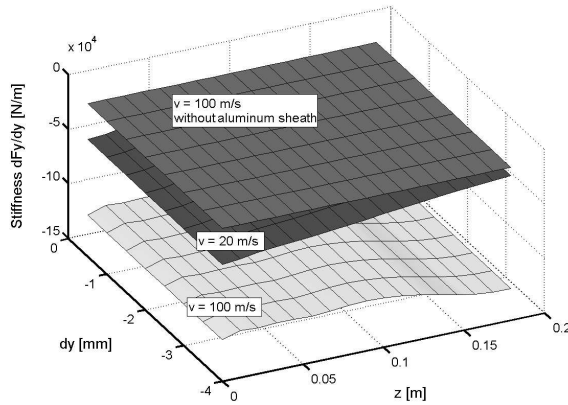


Figure 10. Stiffness $\partial F_y/\partial y$ of a single unit at different speeds of the levitating force F_y as a function of the distance traveled by the vehicle and its vertical shift d_y .

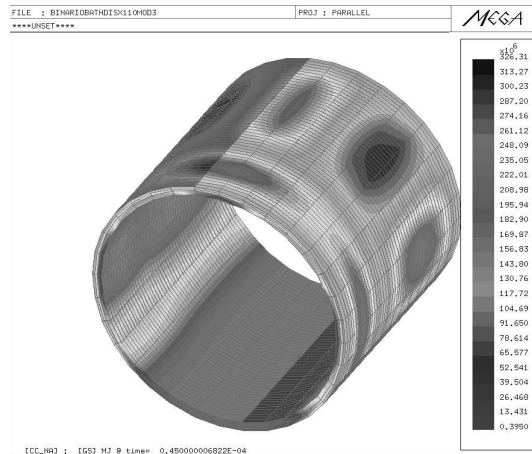


Figure 11. Eddy current density distribution on the aluminum sheath during the motion of the vehicle.

4.2. Thermal Behavior

The analysis of the thermal behavior is necessary since the magnetic properties of a PM strongly depend on temperature. The heat source is related to the ohmic losses due to the induced eddy currents on the aluminum, as reported in Fig. 11.

The thermal model, used to estimate the maximum increase of the aluminum temperature and consequently of the permanent

magnets, has the scalar variable temperature T as the unknown and the governing equation, neglecting convection and radiation, is [26]:

$$\nabla \times \lambda \nabla T - C \frac{\partial T}{\partial t} = -Q \tag{2}$$

where the temperature T is in $^{\circ}\text{K}$, λ the thermal conductivity in $\text{Wm}^{-1}\text{K}^{-1}$, C the heat capacity in $\text{Jkg}^{-1}\text{K}^{-1}$, and $Q = J^2/\sigma$ the heat source density in Wm^{-3} .

Figure 12 shows the profile of temperature increase, as a function of speed, due to the transit of a vehicle system on the rails. Taking into account the total length of the vehicle and assuming the largest shift $d_{x,y}$ from the centered path, which produces the largest intensity of the induced eddy currents, the maximum temperature increase due to eddy currents at $v = 100 \text{ m/s}$ is less than 30°K . At $v = 20 \text{ m/s}$ is 53°K .

Then, taking into account also the variation of the outside temperature, the system could undergo mechanical stresses that can arise because of the different thermal expansion coefficients of the aluminum ($\lambda_{Al} = 24 \times 10^{-6} \text{ }^{\circ}\text{K}^{-1}$) and permanent magnets ($\lambda_{PM} = 4 \times 10^{-6} \text{ }^{\circ}\text{K}^{-1}$). Although a deep analysis would need the use of dedicated thermo/mechanical codes, some preliminary considerations can be carried out.

Let us assume that outside temperature is in the range $[T_1 \div T_2]$, where $T_1 = -20^{\circ}\text{C}$ and $T_2 = 40^{\circ}\text{C}$. The overall temperature variation of the aluminum sheath is $\Delta T_{sheath} = \Delta T + (T_2 - T_1) \simeq 100^{\circ}\text{C}$, where $\Delta T = 40^{\circ}\text{C}$ corresponds to the temperature increase at 40 m/s as shown in Fig. 11. As far as the inner part (PMs and their aluminum

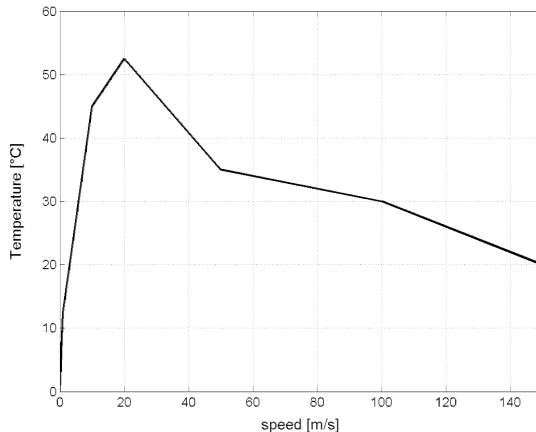


Figure 12. Temperature increase ΔT as a function of the speed.

support), since the eddy currents are negligible, the temperature increase is due only to the outside temperature variation $\Delta T_{inn} = (T_2 - T_1) \simeq 60^\circ\text{C}$. Under these conditions, the radius of the circular crown where the PMs are located is increased of less than $100\ \mu\text{m}$. The interposition of a layer of prestressed elastic material between the aluminum and the permanent magnets could remediate this drawback.

About the direction of the motion, a gap properly interposed between adjacent portions of the rail is enough to compensate the effects of the thermal expansion.

5. ANALYSIS OF THE VEHICLE OSCILLATIONS

While the vehicle is moving along its path, it is affected by external forces that cause the vehicle to shift from its centered trajectory. Such forces, typically discontinuous, due for example to gusts of wind, have to be compensated by internal system forces that tend to bring the vehicle onto its original trajectory.

In order to evaluate the response to the vehicle to the external force we have to integrate the dynamic equation taking into account the inertial force, the external force and the interaction between the vehicle and the rail. We project the dynamic equation in three orthogonal directions neglecting as a first approximation the coupling terms. This is justified by the results obtained in Section 4 and reported in Figs. 5–10, which allow stating that the nature of the forces (levitating in the vertical direction and restoring in the transverse direction) does not change if the vehicle is shifted with respect to the centered position.

When projecting the force along the direction of the motion we have to consider the inertial forces, the drag force (included the electromagnetic drag) and the thrust force. A more detailed analysis will be performed in the next section.

In order to evaluate the amplitude of the vehicle oscillations in the horizontal direction x , we project the Newtons law on this direction. We can write:

$$F_{in} + F_{xr} = F_d \quad (3)$$

where F_{in} represents the inertial force of the whole vehicle, and F_{xr} is the total force between the rails and the vehicle, i.e., the resultant of the interactions between the two systems of PMs and the interactions between the PMs on the vehicle and the eddy current on the rails. The right hand side term F_d represents an external destabilizing force. In the light of the results obtained in Section 3, F_{xr} is a stabilizing force in the speed range of interest. For small values of the deviation x of

the vehicle from its centered trajectory it is possible to express F_{xr} as:

$$F_{xr} \simeq \frac{\partial F_x}{\partial x} \cdot x = K_x \cdot x \quad (4)$$

where K_x is the stiffness of F_x along the x direction. Substituting (4) in (3) yields:

$$M \frac{d^2}{dt^2} x + K_x \cdot x = F_d \quad (5)$$

where M is the total mass of the vehicle. As an example of solution of (5) let us start considering the stationary case characterized by the presence of a constant force F_d in the x direction. Under the applied F_d the vehicle is shifted in the same direction of the quantity: $x_{\max} \simeq F_d/K_x$. We assume that F_d goes suddenly to zero; introducing in (5) the initial conditions: $x(0) = F_d/K_x$ and $v_x(0) = 0$ the solution is:

$$x(t) = x_{\max} \sin(\omega_0 t) \quad (6)$$

where $\omega_0 \simeq \sqrt{K_x/M}$ is the natural frequency of the vehicle oscillations. As a numerical example let us consider a lateral force $F_d = 50$ kN and a stiffness value $K_x = -4 \times 10^7$ N/m, deduced by the results reported in Section 4. We find that the maximum amplitude of the oscillations does not exceed the value $x_{\max} \simeq 1.25$ mm and that the frequency is $f_0 = \omega_0/(2\pi) \simeq 5.8$ Hz. Since such oscillations are small, they can be easily suppressed by the use of a secondary suspension system. Active dampers based on the magnetorheological fluids technology can be advantageously used to increase the comfort of the passengers [40, 41].

The vertical oscillations can be analyzed in the same manner, considering that the interaction force between the rails and the vehicle has a stabilizing effects independently on the presence of the induced current.

6. POWER PROPULSION REQUIREMENTS

The propulsion system should produce a thrust force able to counterbalance all the forces that hinder the motion of the system (in particular aerodynamic and magnetic drag forces) [42]. Aerodynamic drag force increases as the square of the speed, and in our case its value is about 25 kN at 100 m/s; magnetic drag force, instead, decreases inversely with the speed and its value is about 30 kN at 100 m/s. Furthermore, in order to accelerate the vehicle, it is necessary to counterbalance the inertial force which assuming the maximum value of the acceleration $a = 1$ m/s² is: $F_{in} = M \cdot a = 30$ kN. Although at constant cruising speed, the estimated demand of the propulsion power is about 5.5 MW, the propulsion system is required to produce

a proper thrust in order to accelerate the vehicle to its cruising speed. Furthermore an additional propulsion power has to be considered if the vehicle has to travel a slope bringing the a total propulsion power to about 10 MW.

Due to the presence of a small clearance between the rails and the vehicle with respect to other maglev systems, it is possible to reintroduce the use of a linear induction motor in place of a linear synchronous motor that, for different reasons, was gaining in popularity in such systems. The propulsion system could be adapted in tubular shape, also to increase the stiffness of the whole maglev system by exploiting the selfcentering characteristics of the tubular linear induction motors.

7. CONCLUSIONS

In this paper, a controlled passive maglev system has been presented. The use of PMs both on the guideway and on the vehicle assures the suspension of the system. The presence of an aluminum sheath surrounding the rails allows overcoming the intrinsic instability with respect the translations. The thermal behavior has been investigated since high temperatures and intense magnetic fields can damage the PMs. The results have shown that the values of temperature is below the critical threshold for the proposed materials. The analysis of forces and stiffness has shown a good stability of the system under external destabilizing forces. The oscillations resulting by external forces applied along the directions transverse to the motion, are characterized by small amplitude and low frequency. They can be easily suppressed by means of a secondary suspension system. Finally the propulsion power demand has been estimated and a possible use of a tubular linear induction motor as propeller has been briefly indicated. The proposed system seems to be able to satisfy the requisite of a functional Maglev system. Further investigations, taking into account some coupling terms here neglected will be carried on.

REFERENCES

1. Lee, H. W., K. C. Kim, and J. Lee, "Review of maglev train technologies," *IEEE Trans. Magn.*, Vol. 42, No. 7, 1917–1925, Jul. 2006.
2. Eastham, A. R. and W. F. Hayes, "Maglev systems development status," *IEEE Aerosp. Electron. Syst. Mag.*, Vol. 3, No. 1, 21–30, Jan. 1988.
3. Gutberlet, H., "The German magnetic transportation program," *IEEE Trans. Magn.*, Vol. 10, No. 3, 417–420, Sep. 1974.

4. Meins, J., L. Miller, and W. J. Mayer, "The high speed Maglev transport system transrapid," *IEEE Trans. Magn.*, Vol. 24, No. 2, 808–811, Mar. 1988.
5. Ono, M., S. Koga, and H. Ohtsuki, "Japan's superconducting maglev train," *IEEE Trans. Instrum. Meas. Magazine*, Vol. 5, No. 1, 9–15, Mar. 2002.
6. Tsuchiya, M. and H. Ohsaki, "Characteristics of electromagnetic force of EMS-type maglev vehicle using bulk superconductors," *IEEE Trans. Magn.*, Vol. 36, No. 5, 3683–3685, Sep. 2000.
7. Hull, J. R., "Attractive levitation for high-speed ground transport with large guideway clearance and alternating-gradient stabilization," *IEEE Trans. Magn.*, Vol. 25, No. 5, 3272–3274, Sep. 1989.
8. Bohn, G. and G. Steinmetz, "The electromagnetic levitation and guidance technology of the transrapid test facility Emsland," *IEEE Trans. Magn.*, Vol. 20, No. 5, 1666–1671, Sep. 1984.
9. Wang, J., S. Wang, et al., "Guidance forces on high temperature superconducting Maglev test vehicle," *IEEE Trans. Appl. Supercond.*, Vol. 13, No. 2, 2154–2156, Jun. 2003.
10. Wang, S., J. Wang, et al., "The man-loading high-temperature superconducting Maglev test vehicle," *IEEE Trans. Appl. Supercond.*, Vol. 13, No. 2, 2134–2137, Jun. 2003.
11. Sasakawa, T. and N. Tagawa, "Reduction of magnetic field in vehicle of superconducting maglev train," *IEEE Trans. Magn.*, Vol. 36, No. 5, 3676–3679, Sep. 2000.
12. Di Majo, F. and G. Sciarrone, "The future of the very high speed transportations," *CSST*, CNR, Rome, 1987.
13. Ausserlechner, U., "Closed analytical formulae for multi-pole magnetic rings," *Progress In Electromagnetics Research B*, Vol. 38, 71–105, 2012.
14. Babic, S. and C. Akyel, "Magnetic force between inclined circular loops (Lorentz approach)," *Progress In Electromagnetics Research B*, Vol. 38, 333–349, 2012.
15. Ravaud, R., G. Lemarquand, and V. Lemarquand, "Halbach structures for permanent magnets bearings," *Progress In Electromagnetic Research M*, Vol. 14, 263–277, 2010.
16. Janssen, J. L. G., J. J. H. Paulides, and E. A. Lomonova, "Study of magnetic gravity compensator topologies using an abstraction in the analytical interaction equations," *Progress In Electromagnetics Research*, Vol. 128, 75–90, 2012.
17. Earnshaw, S., "On the nature of molecular forces which regulate

- the constitution of luminofeorous ether,” *Trans. Comb. Phil. Soc.*, Vol. 7, 97–112, 1842.
18. Braunbek, W., “Freischwebende korper in elektishen und magnetishen feld,” *Z. Phisik*, Vol. 112, 753–763, 1939.
 19. Bassani, R., “Permanent magnetic levitation and stability,” *Proceedings of NATO Advanced Study Institute on Fundamentals of Tribology etc.*, 899–913, Kluwer Academic Publishers, 2000.
 20. Bassani, R., E. Ciulli, F. Di Puccio, and A. Musolino, “Study of conic permanent magnet bearings,” *Meccanica*, Vol. 36, No. 6, 745–754, 2001.
 21. Bekinal, S. I., T. R. Anil, and S. Jana, “Analysis of axially magnetized permanent magnet bearing characteristics,” *Progress In Electromagnetics Research B*, Vol. 44, 327–343, 2012.
 22. Tozoni, O. V., “New stable magnetodynamic suspension system,” *IEEE Trans. Magn.*, Vol. 35, No. 2, 1047–1054, Mar. 1999.
 23. Paudel, N., S. Paul, and J. Z. Bird, “General 2-D transient eddy current force equations for a magnetic source moving above a conductive plate,” *Progress In Electromagnetics Research B*, Vol. 43, 255–277, 2012.
 24. Tokoro, H. and K. Uchida, “High energy product Nd-Fe-B sintered magnets produced by wet compacting process,” *IEEE Trans. Magn.* Vol. 37, 2463–2466, Jul. 2001.
 25. Matrosov, V. M., et al., “A new passive maglev system based on eddy current stabilization,” *IEEE Trans. Magn.*, Vol. 45, No. 3, 984–987, Mar. 2009.
 26. EFFE, User manual, Bathwick Electrical Design Ltd, UK, Sep. 2009.
 27. MAGNET, <http://www.infolytica.com/en/products/magnet/>, 2012.
 28. Musolino, A. and R. Rizzo, “Numerical analysis of brush commutation in helical coil electromagnetic launchers,” *IET Science, Measurement and Technology*, Vol. 5, No. 4, 147–154, Jul. 2011.
 29. Musolino, A. and R. Rizzo, “Numerical modeling of helical launchers,” *IEEE Trans. Plasma Sci.*, Vol. 39, No. 3, 935–940, Mar. 2011.
 30. Barmada, S., et al., “Force and torque evaluation in hybrid FEM-MOM formulations,” *IEEE Trans. Magn.*, Vol. 37, No. 5, 3108–3111, Sep. 2001.
 31. Tripodi, E., et al., “Modeling of electromechanical devices by GPU-accelerated integral formulation,” *Int. J. Numer.*

- Model.*, 1–21, Published online in Wiley Online Library (wileyonlinelibrary.com), 2012, DOI:10.1002/jnm.1860.
32. Tripodi, E., et al., “Acceleration of electromagnetic launchers modeling by using graphic processing unit,” *IEEE 16th EML Symposium Conference Proceedings*, 1–6, Beijing, May 15–19, 2012.
 33. Musolino, A., “Finite-element method/method of moments formulation for the analysis of current distribution in rail launchers,” *IEEE Trans. Magn.*, Vol. 41, No. 1, 387–392, 2005.
 34. Raugi, M., et al., “3-D field analysis in tubular induction launchers with armature transverse motion,” *IEEE Trans. Magn.*, Vol. 35, No. 1, 154–159, 1999.
 35. Rizzo, R., et al., “Numerical simulation of a complete generator-rail launch system,” *IEEE Trans. Magn.*, Vol. 41, No. 1, 369–374, 2005.
 36. Rizzo, R., et al., “Analysis of the performance of a combined coil-rail launcher,” *IEEE Trans. Magn.*, Vol. 39, No. 1, 103–107, 2003.
 37. Raugi, M., et al., “Analysis of the performance of a multi-stage pulsed linear induction launcher,” *IEEE Trans. Magn.*, Vol. 37, No. 1, 111–115, Jan. 2001.
 38. Tucci, M., et al., “A wavelet based method for the analysis of impulsive noise due to switch commutations in Power Line Communication (PLC) systems,” *IEEE Trans. Smart Grid*, Vol. 2, No. 1, 80–89, Mar. 2011.
 39. Tucci, M., et al. “Multi-resolution based sensitivity analysis of complex non-linear circuits,” *IET Circuits, Devices and Systems*, Vol. 6, No. 3, 176–186, 2012.
 40. Jiang, Z. and R. E. Christenson, “A fully dynamic magneto-rheological fluid damper model,” *IOP Smart Mater. Struct.*, Vol. 21, 1–12, May 2012.
 41. Bicchi, A., et al., “Electromagnetic modeling and design of haptic interface prototypes based on magnetorheological fluids,” *IEEE Trans. Magn.*, Vol. 43, No. 9, 3586–3599, Sep. 2007.
 42. Yan, L., “Suggestion for selection of maglev option for Beijing-Shanghai high-speed line,” *IEEE Trans. Appl. Supercond.*, Vol. 14, No. 2, 936–939, Jun. 2004.